Chemical Engineering Journal 285 (2016) 331–340

Contents lists available at ScienceDirect

Chemical Engineering Journal

journal homepage: www.elsevier.com/locate/cej

Kinetics of CO_2 and steam gasification of Victorian brown coal chars

Joanne Tanner, Sankar Bhattacharya *

Department of Chemical Engineering, Monash University, Wellington Rd, Clayton 3800, Australia

HIGHLIGHTS

- Char prepared by rapid pyrolysis at 1000 °C in a drop tube furnace.
- Thermogravimetric analysis under CO_2 and H_2O between 650 and 1100 °C.
- Intrinsic kinetic parameters determined by data fitting and Arrhenius analysis.
- Mass transfer limitations (Regime I to II transition) observed from fitted data.
- Char morphology, Na and Ca content greatly influence char gasification kinetics.

GRAPHICAL ABSTRACT

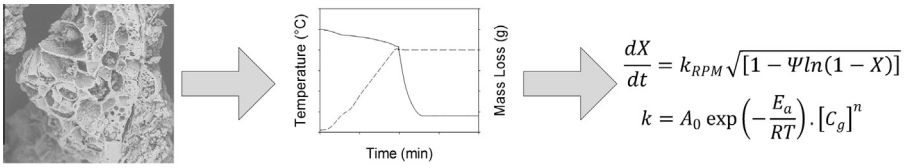

Char Preparation
100% N_2
1000 °C
6 seconds

TG Analysis
30 – 90% CO_2/N_2
30 – 70% H_2O/N_2
650 – 1100 °C

Kinetic Modelling
Activation Energy, E_a
Frequency Factor, A_0
Reaction Order, n

ARTICLE INFO

Article history:
Received 11 June 2015
Received in revised form 19 September 2015
Accepted 29 September 2015
Available online 13 October 2015

Keywords:
Victorian brown coal
Gasification kinetics
Reactivity

ABSTRACT

This work reports a kinetic study of the CO_2 and steam gasification of Victorian brown coal chars produced by rapid pyrolysis in a vertical drop tube furnace under entrained flow conditions. The study was performed by atmospheric pressure thermogravimetry over a temperature range of 650–1100 °C. The intrinsic kinetic parameters for the chemical rate control regime were determined, and the onset temperature of mass transfer limitations observed. The experimental results were well described by the volumetric model, grain model and random pore model for char conversion from 10% to 50% due to the high porosity created during rapid pyrolysis. Activation energies ranging from 162 to 175 kJ/mol and 119 to 165 kJ/mol were determined for CO_2 and steam gasification of Morwell, Loy Yang and Yallourn coal chars, respectively. The pre-exponential factors were of similar orders of magnitude, and increased for a smaller particle size range. The instantaneous relative reactivities, $k(H_2O)/k(CO_2)$, at 800 °C for the three Victorian brown coal chars ranged from 1.2 to 2.5, indicating a significant influence of the partial pressure of gasification reagent. The dominant influence in the case of CO_2 gasification reactivity of these chars appears to be similar for all three coals and is morphological in nature. The order of increasing activation energies for char-steam gasification correlated well with the molar ratio Na/(Ca + Na) in the char.

1. Introduction

An increasing worldwide demand for energy, as well as chemical and petrochemical products, has led to renewed interest in the generation of syngas via coal gasification as an adaptable, alternate feedstock for these applications [1]. Syngas from low rank coals is of particular interest for countries with large domestic resources; however, there is little data available regarding the use of state of the art entrained flow gasification technologies with low rank coals. Gasification is a complex chemical process, and an enhanced understanding of fundamental reaction kinetics and reactivity under controlled laboratory conditions to support larger scale gasification trials contributes to a greater understanding of the

* Corresponding author. Tel.: +61 3 9905 9623; fax: +61 3 9905 5686.
E-mail address: sankar.bhattacharya@monash.edu (S. Bhattacharya).

http://dx.doi.org/10.1016/j.cej.2015.09.106
1385-8947/

Nomenclature

A_0	Arrhenius equation pre-exponential factor
C_g	concentration of the gasifying agent (CO_2 or steam)
E_A	apparent activation energy
E_t	true activation energy
ε_0	initial particle porosity
$f(X)$	structure factor accounting for the dependence of char structure on conversion
$k(C_g,T_p)$	generic char reaction rate at gas concentration C_g and particle temperature T_p
k_{GM}	grain model reaction rate
k_{RPM}	random pore model reaction rate
k_{VM}	volumetric model reaction rate
L_0	initial length of all particle pores per unit volume
m_0	mass of dry, ash-free char at time = 0
m_t	mass of dry, ash-free char at time = t
m	true reaction order with respect to the gasifying agent (CO_2 or steam)
n	apparent reaction order with respect to the gasifying agent (CO_2 or steam)
Ψ	dimensionless structural correlation for the random pore model
S_0	initial char surface area per unit volume
t	time
T_p	particle temperature
X	char conversion

underlying chemistry [2]. Furthermore, once the fundamental parameters are known, the process may easily be modelled from the desired reaction conditions including temperature, pressure, and atmospheric composition. It is therefore important to determine the kinetic parameters for various applicable scenarios, such that modelling may henceforth be used to predict the gasification behaviour under various analogous conditions.

Coal gasification may be generally described as the two-step process of rapid devolatilisation followed by protracted gasification of the nascent char. The parameters of the devolatilisation step affect the subsequent rate limiting char gasification step. Char gasification reactivity is therefore fundamental to the process, and is a complex function of the parent coal properties, the char properties, and the gasification conditions [3]. As such, char gasification reactivity requires extensive investigation under standardised conditions in order to determine the kinetic parameters for various scenarios of industrial applicability. Numerous publications detailing the general effects of various intrinsic and experimental parameters on char gasification reactivity [4–6] indicate that the most influential parameters are the structure and thermal history of the char, and the chemical composition of the parent coal.

Char physical characteristics, including surface area, concentration of active sites at the surface, porosity and interconnectivity of the pore structure, contribute to differences in char gasification reactivity. The heating rate, temperature and duration of devolatilisation, in combination with the parent coal properties, influence these char characteristics. Rapid devolatilisation at high temperatures, high heating rates and low residence times results in a highly reactive, high porosity char with interconnected pore structure [7]. Conversely, slow devolatilisation results in annealing of the char, reducing char gasification reactivity by the gradual rearrangement of its constituent hydrocarbon structures [8–10]. The rank of the parent coal, particularly in terms of volatile matter and macerals, also influences the resulting char characteristics as the conditions affect the behaviour of these constituents during devolatilisation. In addition, char morphology evolves continuously during gasification due to further annealing and the influence of the reagent gas. Steam, in particular, has a marked influence on the evolution of char structure during gasification. Hydrogen radicals produced as intermediate species during the steam gasification mechanism induce condensation reactions in the char, altering the char morphology as gasification progresses [3,11].

In addition to the char physical characteristics, apparent char gasification reactivity is also necessarily a function of the two fundamental heterogeneous reactions occurring at the char surface, i.e., the char-CO_2 and char-steam gasification reactions:

$$C_{(s)} + CO_{2(g)} \leftrightarrow 2CO_{(g)} \quad \Delta H = +172.7\ \text{kJ/mol}$$

$$C_{(s)} + H_2O_{(g)} \leftrightarrow H_{2(g)} + CO_{(g)} \quad \Delta H = +131.5\ \text{kJ/mol}$$

The kinetics of these reactions are well known to be catalysed at low and intermediate temperatures by inherent inorganic species in the parent coal, which are retained in the devolatilised char [3,5]. Low rank coals contain inorganic species which have the potential to catalyse char gasification reactions including alkali (Na, K), alkaline earth (Ca, Mg) and transition metals (Fe). The proposed mechanisms involve redox cycles of the catalytic species and are discussed in detail elsewhere [12]. These species are present within the coal structure as hydrated cations within the pore water, cations bound to the coal surface as carboxylates, and rarely as discrete mineral inclusions [13]. The catalytic Na, K, Ca, Mg and Fe species remain in the char in highly dispersed forms upon devolatilisation. The catalytic activity of these species under CO_2 and steam gasification conditions decreases with increasing temperature due to the increasing influence of mass transfer effects over chemical rate control, and increased volatilisation of the inorganic species, in particular Na, which is essentially absent in char produced at temperatures above 1000 °C [14].

Fig. 1 shows the general dependence of char gasification reaction rate on temperature. At low temperatures, the apparent rate is controlled by the heterogeneous reaction between solid carbon from the char and a gas phase reagent, being either CO_2 or steam (Regime I). As temperature increases and approaches the transition to Regime II, typically at around 1000 °C, the rate of chemical reaction increases such that the rate of diffusion of reagent gases

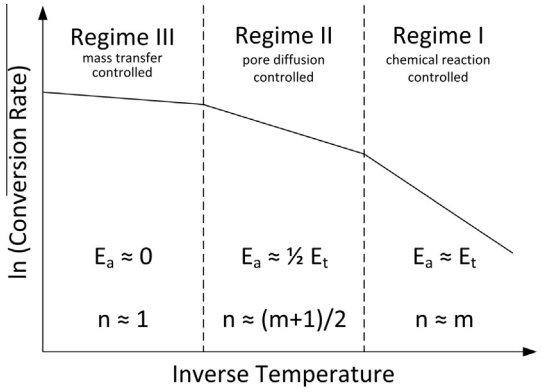

Fig. 1. The change in reaction rate of a porous carbon with temperature (adapted from [15]).

through the pore structure to reactive carbon sites begins to influence the overall rate of char conversion [15]. The transition between Regime I and II therefore signifies the onset of diffusion limitations, and may be observed in experimental studies by the variation in the temperature dependence of the reaction rate, as temperature has a marked influence on the rate of the endothermic char gasification reactions, but comparatively little impact on gas diffusion through pores. Modern coal gasification processes are typically based on entrained flow gasification technologies in the temperature range of 1200–1600 °C. The depicted transition to Regime III, where the gasification rate is limited by the rate of diffusion of the reagent gas through the boundary layer surrounding the char particle, typically occurs in excess of 1500 °C. Therefore, this transition may not occur under entrained flow conditions [16].

Thus it is clear that the production and kinetic characterisation of coal chars under industrially relevant laboratory conditions is by no means a trivial subject. Thermogravimetric analysis (TGA) is widely used in the measurement of char gasification kinetics [17] in the absence of any external mass transfer or pore diffusion limitations, i.e., under Regime I kinetic conditions. This technique is therefore useful in determining both the chemical reaction kinetics, and also the transition temperature range between chemical rate control and pore diffusion control regimes [18].

There has recently been a renewed interest in low rank coal-to-products processes via gasification, particularly for areas with significant domestic resources, such as the state of Victoria, Australia. The low rank coals in this region are known as brown coals, and are used almost exclusively for mine-mouth pulverised combustion power generation. However, this world class resource also presents a significant potential for use in coal-to-products gasification processes. In order to evaluate, compare, model and optimise the coal gasification process, fundamental data relating to the chemical reactions, including reaction kinetics, is required. Comprehensive, comparative gasification kinetics data on Victorian brown coals is unavailable. As it is not practicable to use previously obtained data for other low rank coals, this study has therefore been undertaken to investigate the kinetics of Victorian brown coal gasification. In order to decouple the intrinsic chemical reaction described by Regime I kinetics from the diffusion-affected Regime II kinetics observed at higher temperatures, a series of char gasification experiments was performed. Char samples from Morwell, Loy Yang and Yallourn coals were prepared under rapid pyrolysis conditions representative of the industrial gasification process. The char was sized to 38–53 μm and 90–106 μm fractions, and the six samples subjected to a series of thermogravimetric analysis experiments under CO_2 and steam gasification conditions between 650 °C and 1100 °C. The kinetic parameters were determined using an nth order Arrhenius equation and the Regime I – Regime II transition temperature range determined graphically. These data contribute directly to process models for the prediction of coal gasification behaviour under conditions of industrial interest, and therefore to the design and optimisation of industrial gasification applications.

2. Materials and methods

2.1. Sample preparation

Three Victorian brown coals were considered in this study, sourced from the Morwell, Yallourn, and Loy Yang open cut mines. The samples were air-dried, pulverised and sieved to <150 μm. The preparation of char for the kinetics study was performed in an electric drop tube furnace (DTF) operated under 100% nitrogen at 1000 °C. The apparatus is depicted and described in further detail elsewhere [19]. A total gas flowrate of 5 L/min was maintained, with 10% directed to purge the vibratory feed system and the balance delivered to the reactor via the annular preheating space. Char samples were sieved to the required particle size fractions and stored in sealed containers at room temperature prior to thermogravimetric analysis. The particle residence time during pyrolysis was approximately 6 s [19].

Initially, a char particle size range of 90–106 μm was chosen as representative of the industrial entrained flow gasification process; however, Dynamic Light Scattering (DLS) analysis of the particle size distribution of the bulk DTF char indicated that rapid pyrolysis shifts the size range of the resultant char to smaller particle sizes than the feed coal. Furthermore, it is well known that there is a char-specific size range below which pore diffusion restrictions may be neglected [4], and that catalytic elements are generally concentrated in smaller particles [8]. Preliminary TGA experiments indicated that diffusion restrictions exist for Morwell coal char above a size range of 75–90 μm. Therefore, a series of duplicate preparations and experiments were also performed using 38–53 μm char in order to determine the effect of particle size on gasification kinetics at small, narrow particle size ranges.

The parent coal and char samples were characterised by a number of standard methods. Air-dried moisture and proximate analysis were performed according to Australian Standard Series 2434 – Methods for the analysis and testing of lower rank coal and its chars. Ultimate analysis was performed using a Perkin-Elmer 2400 Series II CHNS/O System. Elemental analysis was performed by ICP-OES following borate fusion and acid dissolution according to AS 1038.14.1-2003 (R2013) using low temperature ash, prepared in a muffle furnace at 500 °C, from the coal and char samples. CO_2 adsorption measurements were performed on a Micromeretics ASAP 2020 instrument and the corresponding char surface areas calculated by the Dubinin–Radushkevich isotherm. Density and porosity measurements were performed using a Micromeretics Autopore IV Mercury Porosimeter. Scanning electron microscopy (SEM) images were obtained using a Phenom Pro Desktop SEM. The results of the chemical and physicochemical analysis are presented in Tables 1–4.

Uncharacteristically high ash, aluminium and silicon were measured in the Loy Yang coal sample, and the presence of large amounts of crystalline silica in the ash was confirmed by XRD. It is therefore likely that sand or clay has been included during sample collection. The effect on the char gasification reactivity is likely to be minimal due to the relatively inert form of the inclusions. Some portion is clearly available to capture S and Na, however, as evidenced by the accumulation of these elements in the char (Table 2).

2.2. Thermogravimetric analysis

TGA was performed using a Netzsch STA 449 F3 Jupiter instrument to determine the isothermal rate of reaction of each of the prepared coal chars under CO_2 and steam at temperatures between 650 and 1100 °C. This temperature range was chosen such that the kinetic parameters under lower temperature, Regime I conditions, as well as the transition temperature range to Regime II conditions could be determined. Concentrations of 90% CO_2 and 70% steam were chosen, within the bounds of instrument constraints, to eliminate the effect of a limiting reagent on the char gasification reactivity. A gas flowrate of 100 mL/min was chosen to maintain the desired reagent concentration in the TGA and to ensure the rapid removal of product gases known to inhibit the char gasification reactions [20]. The experiments were performed using a thin layer of char (10.5 ± 0.5 mg) in an alumina crucible of 18 mm diameter, 2 mm wall height and 0.5 mm thickness to minimise the effects of gas diffusion and sample temperature lag and gradient [21].

Table 1
Chemical analysis of Victorian brown coal and brown coal char samples.

Sample	Moisture (air dried, wt%)	Proximate analysis (dry basis, wt%)			Ultimate analysis (dry basis, wt%)			
		Ash	Volatile matter	Fixed carbon*	C	H	N	S
Morwell								
Coal	14.92	3.59	49.31	47.10	61.6	4.70	1.55	0.882
Char	3.98	5.64	–	94.36	81.4	1.03	0.71	0.119
Yallourn								
Coal	15.54	2.29	52.16	45.56	60.0	4.95	2.03	1.041
Char	4.19	6.54	–	89.27	87.3	1.11	0.85	0.095
Loy Yang								
Coal	11.16	7.99	48.25	43.76	54.4	4.26	1.01	0.839
Char	3.97	15.53	–	84.47	81.9	1.05	0.68	0.290

* By difference.

Table 2
Ash analysis of the air dried coal and char samples ashed at 500 °C and expressed as % oxide in ash.

Sample	Na_2O	MgO	Al_2O_3	SiO_2	SO_3	K_2O	CaO	TiO_2	Fe_2O_3
Morwell									
Coal	3.70	16.40	0.80	1.50	17.10	0.36	29.00	0.08	12.60
Char	0.09	19.07	1.57	1.31	15.72	0.05	35.53	0.09	15.45
Yallourn									
Coal	4.50	12.00	2.20	19.00	11.70	0.35	6.80	0.11	35.00
Char	3.14	16.27	2.27	1.89	16.47	0.58	7.82	0.11	42.05
Loy Yang									
Coal	1.20	0.90	7.40	78.90	2.30	0.39	0.43	0.68	1.40
Char	3.72	8.29	13.03	34.01	14.47	0.55	8.17	1.26	10.20

Table 3
Selected elemental analysis expressed as mmol/g char and selected molar ratios.

Sample	Na	Ca	Na/(Na + Ca)
Morwell			
Char	0.1595	35.7401	0.0044
Yallourn			
Char	6.6259	9.1177	0.4207
Loy Yang			
Char	18.6322	22.6126	0.4517

A typical experiment proceeded as follows: After an initial ramp at 5 °C/min to 200 °C to drive off residual and adsorbed moisture, the sample was heated at 10 °C/min to 800 °C and equilibrated for 5 min to avoid further thermal lag. The reagent gas was introduced and the gasification reaction proceeded to completion under isothermal conditions. Analogous blank corrections were performed for each temperature-atmosphere combination and subtracted from the sample measurement data to negate instrument effects such as balance drift, gas buoyancy changes, and temperature gradients between the sample and the furnace.

3. Results and discussion

In this section, Morwell results have been used to graphically demonstrate the analytical process and validity of the chosen models to represent the experimental data. The measurements, data fitting and correlations for Loy Yang and Yallourn are similar in all cases; therefore only the numerical results are included for these samples.

Table 4
Physical properties of the char samples.

Char sample	Morwell	Yallourn	Loy Yang
CO_2 surface area (m^2/g)	503.52	630.20	612.11
Hg porosity (%)	76.56	83.96	76.92

Thermogravimetric analysis data for char gasification take the general form of mass loss over time for a specified temperature profile. In this investigation, a series of isothermal experiments under CO_2 and steam atmospheres at temperatures between 650 and 1100 °C were performed. The mass loss data from each isothermal experiment was blank corrected and smoothed using the Netzsch Proteus Analysis 5.1 software package. The gasification segment was exported and normalised from 0% to 100% char conversion on an ash free basis according to Eq. (1).

$$X = \frac{m_0 - m_t}{m_0} \tag{1}$$

The processed conversion results for Morwell coal char are presented in Fig. 2. The time scale has been truncated to better display the high temperature data.

As expected, the conversion rate increased with increasing temperature; hence the plots converge at high temperature. The temperature range of convergence coincides with the onset of mass transfer effects, i.e., the transition between Regime I and Regime II in Fig. 1. Experiments performed above this critical temperature therefore exhibit coinciding results due to the nature of the experimental design, which eliminates all factors affecting the reaction rate under low temperature conditions except the chemical reaction itself, thereby showing the effect of reactive gas diffusion limitations at higher temperatures.

For the same particle size range, the char conversion rate for analogous experiments in steam increased, indicating that the char reactivity in steam was higher than in CO_2 [15]. The reaction rate of the 38–53 μm particle size fraction was slightly lower than that of the 90–106 μm size fraction based on the normalised char conversion plots, but the difference is considered negligible.

3.1. Model fitting

The instantaneous char conversion rate at any point during a gasification reaction can be described by the general expression given in Eq. (2) [22].

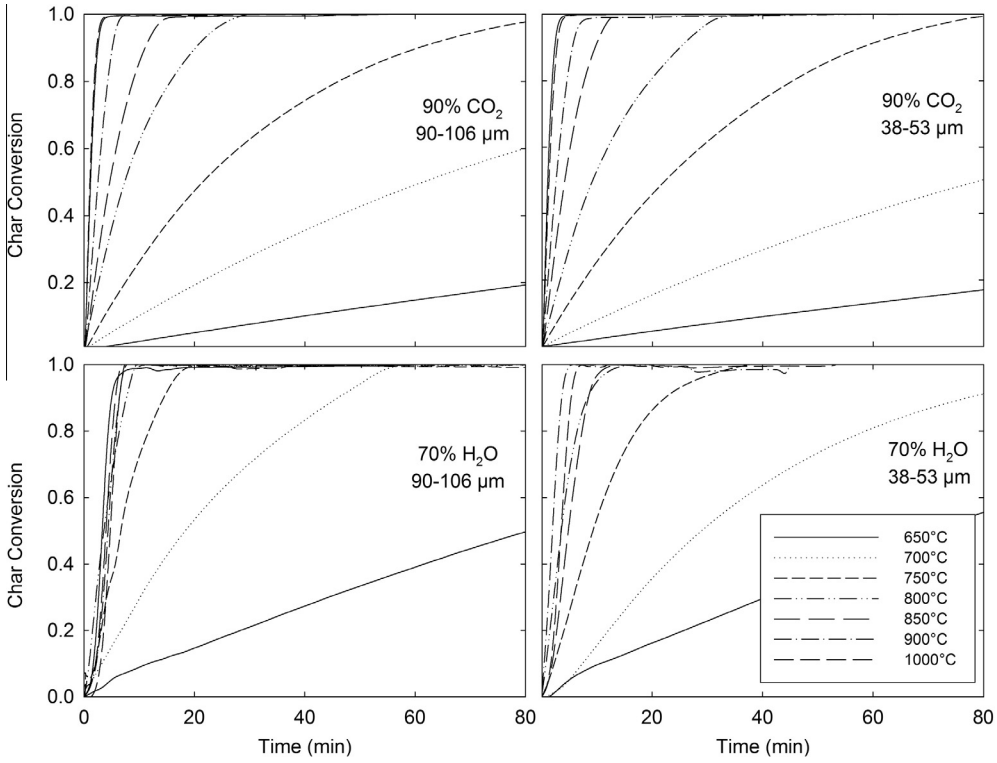

Fig. 2. Char conversion versus time for CO_2 and steam gasification of 38–53 µm and 90–106 µm Morwell char particle size fractions at various temperatures.

$$\frac{dX}{dt} = k(C_g, T_p)f(X) \tag{2}$$

$f(X)$ describes the changes in physical or chemical properties of the char as the reaction proceeds, and may be modelled with varying degrees of accuracy depending on the associated assumptions made regarding the nature and structure of the char. $k(C_g, T_p)$ is the intrinsic surface reaction rate, and follows Langmuir–Hinshelwood (LH) reaction kinetics for CO_2 and steam gasification of coal chars at atmospheric pressure [11,23]. However, due to the complexity of fundamental LH modelling, the effects of temperature and reagent partial pressure on char gasification rates are typically modelled using an nth order rate equation.

In this study, $\frac{dX}{dt}$ was therefore measured experimentally by TGA, and used to calculate the rate constant k, as well as the kinetic parameters of the rate equation applicable to the conditions of interest. Three common gas–solid models were chosen to fit the experimental char conversion data and so to describe the $f(X)$ term in Eq. (2). Details of these models and their corresponding equations are presented in Table 5.

The three models differ primarily in the assumptions made regarding the particle structure and hence reactive site locations. The volumetric model (VM), also known as the homogeneous model, is commonly used to simplify heterogeneous reaction kinetics in cases where it may be assumed that the chemical reaction is taking place simultaneously at all points within the particle. The grain model (GM), also known as the shrinking core model, assumes that the particle is a solid sphere, and that the chemical reaction is occurring at the outer surface only. The random pore model (RPM), as the name suggests, considers a randomly overlapping pore structure. Accordingly, the VM and GM do not account for any variation in internal structural factors with conversion, where the RPM considers the evolution of char structure as gasification proceeds.

There are many other models which have also been proposed to account for deviations from these standard models. They include adjustments to account for surface area [24]; char type, heat treatment temperature and active surface area [25]; and the ratio of initial to instantaneous pore surface area [26], among others. Each of these models can be simplified under particular conditions or assumptions to obtain one of the three models given in Table 5.

The RPM is reported as the most commonly used conversion model for kinetic experimental data due to its ability to model the maximum reaction rate often observed in the initial stages of gasification during TG analysis. It has recently been shown, however, that this false maximum is an artefact of the experimental setup, and relates purely to the change in gas atmosphere and subsequent equilibration [28]. Therefore, a lower limit of 10%

Table 5
Summary of char conversion models [4,27].

Model	Separable form	Linear form
Volumetric model (VM)	$\frac{dX}{dt} = k_{VM}(1-X)$	$k_{VM}t = -\ln(1-X)$
Grain model (GM)	$\frac{dX}{dt} = k_{GM}(1-X)^{\frac{2}{3}}$	$k_{GM}t = 3\left[1-(1-X)^{\frac{1}{3}}\right]$
Random pore model (RPM)	$\frac{dX}{dt} = k_{RPM}\sqrt{[1-\Psi ln(1-X)]}$	$k_{RPM}t = \frac{2}{\Psi}[\sqrt{1-\Psi\ln(1-X)}-1]$ where: $\Psi = \frac{4\pi L_0(1-\varepsilon_0)}{S_0^2}$

conversion was chosen for the fitted data based on the estimated time for atmospheric equilibration in the TGA following introduction of the gasification reagent (CO_2 or steam).

An upper limit of 50% conversion was chosen based on the known factors having a detrimental effect on char gasification rate at higher conversions. Over time, carbonaceous material remaining in the char is gradually annealed. Annealing reduces char reactivity by increasing the ordering of the char structure, destroying carbon edges, and reducing structural defects [8–10]. As carbon is simultaneously depleted from the char, micropores coalesce into meso and macropores, reducing char reactivity by effectively reducing the available surface area for gasification [29]. Finally, deactivation of the inherent catalytic inorganic species occurs over time [12]. As conversion increases, each of these interrelated processes has an increasing effect on the gradually decelerating gasification rate, and the experimental data begins to deviate from the ideality of the models. For all char samples, significant deviation was observed for char conversions above 50%, hence this value of X was chosen as the upper limit for subsequent data analysis.

The exclusion of the initial 10% of the data from the analysis also increases the similarity of fit between the three models, as the RPM is the only model which can accurately describe the false maximum which is generally observed in this conversion range [28]. In this study, despite the deliberate elimination of the maximum rate data for which it was developed, the RPM was chosen for use in subsequent data analysis for its higher degree of theoretical sophistication with regards to porosity and pore structure. Furthermore, the RPM narrowly has the highest correlation.

Fig. 3 shows model correlations with selected experimental data between 10% and 50% char conversion. Fig. 3a shows that the data correlates well with all three models. Fig. 3b shows the fit of the RPM to experimental results at varying temperatures within Regime I. The RPM was used to fit the experimental data for each char-temperature-atmosphere combination (Fig. 3b), and k_{RPM} was determined from the gradient of the fitted lines. The model shows high correlation up to 900 °C, indicating that these are intrinsic chemical rate results as intended, i.e., no mass transfer effects are influencing the measured gasification rate. The model correlation at temperatures of 1000 °C and 1100 °C is also acceptable within the 10–50% char conversion range, confirming that the high porosity and open structure of the char allows for relatively easy access to the internal structure. It should be noted that the structural parameter, Ψ, in the RPM was treated as a fitting parameter due to the relative difficulty of obtaining accurate values for the average pore length, L_0. A similar value of approximately 1.4 was determined by regression optimisation for all char samples under all conditions. This congruence provides further evidence that the char structure does not play an important role in the char gasification kinetics for these samples.

The relative reactivities, $k(H_2O)/k(CO_2)$, at 800 °C for the three Victorian brown coal chars ranged from 1.2 to 2.5. This is the same order of magnitude as reported in the classic review by Walker [15], who reported a general char relative reactivity of 3 and a subsequent Victorian brown coal char analysis [30] with a relative reactivity of 2.

As previously mentioned, the RPM narrowly has the highest correlation. A comparison of the assumptions upon which each model is based, in the context of the physical characterisation of the char samples (Table 4) indicates that the similarity of fit is due partly to the similarly high porosity of the three char samples, and to the pore structure itself. Fig. 4 shows SEM images of selected char particles produced by rapid pyrolysis in the DTF. The heterogeneous nature of the coals, and hence of the chars produced therefrom, results in a variety of char structures within a single sample, commonly classified into groups based on their porosity and morphology. Group I particles are highly porous, thin walled and predominantly hollow with a porosity greater than 70%. Group II particles are of medium wall thickness, with porosity between 40% and 70%. Group III particles are denser, and have porosity less than 40% [31].

Fig. 5 shows the internal pore structure of a typical Group II char particle. The highly porous nature of the char is clearly visible in the image, and there are significant interpore connections, enabling rapid gas diffusion to and from the internal surfaces. The majority of particles observed in all samples were visually categorised as Group II, with approximately 10% visually categorised as Group I. These observations compliment the measured porosity of the bulk samples of 76–84% (Table 4). Due to high porosity and pore accessibility of the char particles, the surface area and active carbon sites in the char are highly accessible; therefore char structure appears to have a minimal effect on the gasification reactivity, leading to the similar fit observed for the three conversion models.

3.2. Determination, analysis and comparison of kinetic parameters

For constant reagent concentration conditions, the char gasification rate is dependent on temperature according to the Arrhenius relationship:

$$k = A_0 \exp\left(-\frac{E_a}{RT}\right) \tag{3}$$

In order for chemical reaction to occur, a molecular collision with the correct orientation and sufficient energy to overcome the activation energy barrier is required, i.e., not all collisions in

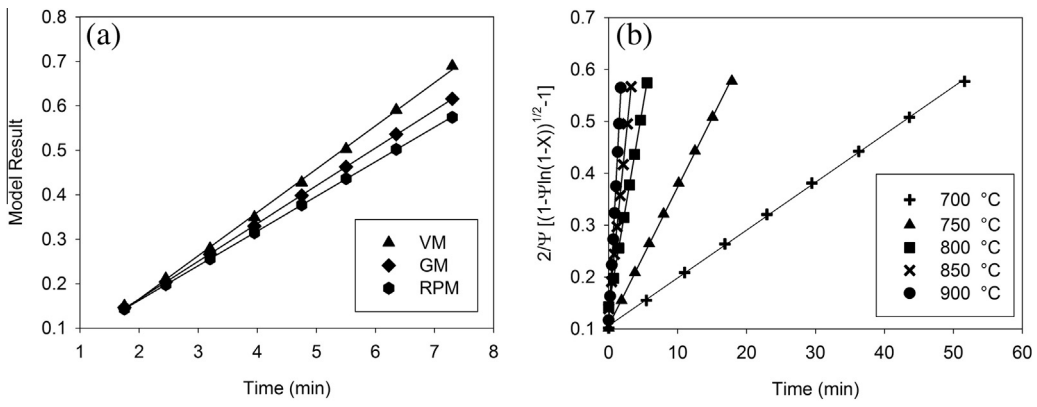

Fig. 3. Correlation of kinetic models to the experimental data for CO_2 gasification of 90–106 μm Morwell char for char conversion from 10% to 50%. (a) Fit of experimental results at 800 °C for the three structural models and (b) Fit of experimental results to the RPM at various temperatures up to 900 °C.

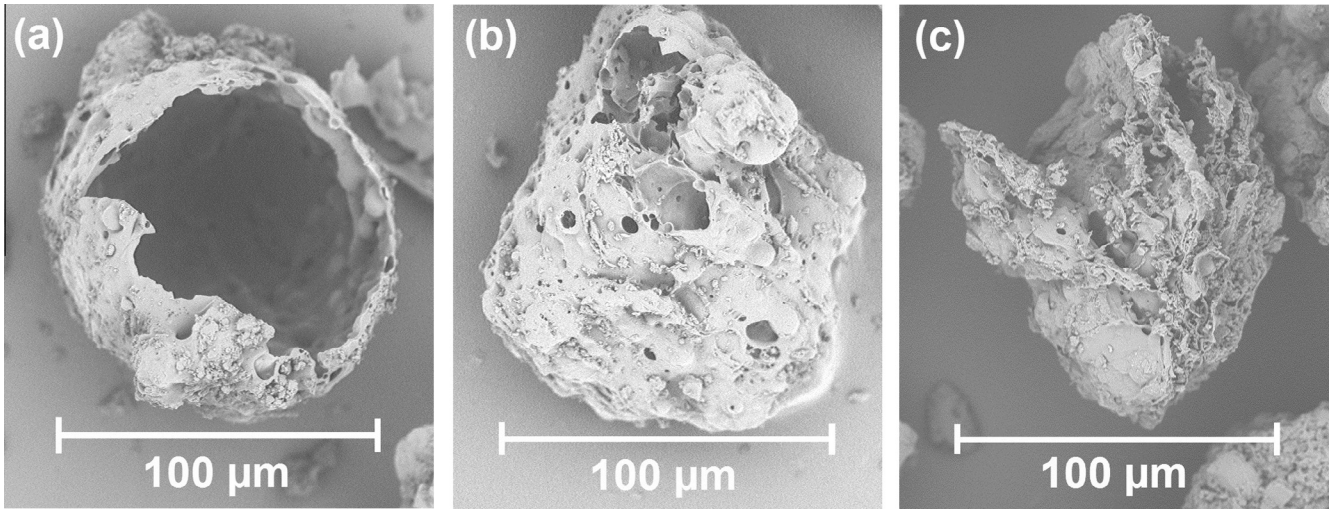

Fig. 4. SEM images showing typical pore structures (a) Group I particle (b) & (c) Group II particles.

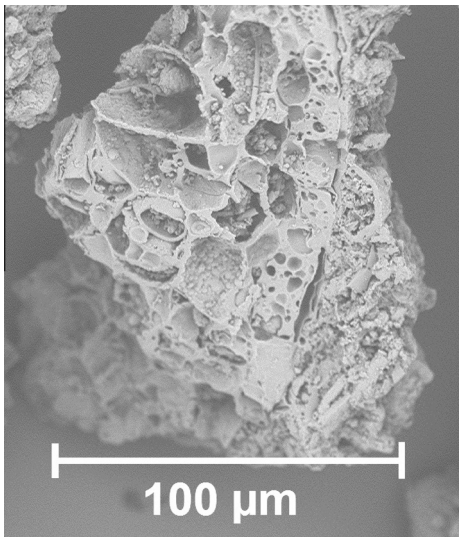

Fig. 5. SEM image showing a cross section and pore structure of a Group II particle of Yallourn char.

the correct orientation, nor all collisions of sufficient energy, result in a chemical reaction. The activation energy, E_a, represents the minimum amount of energy input required to initiate a particular chemical reaction; in this case char-CO_2 or char-steam gasification. The pre-exponential factor, A_0, in the Arrhenius equation is a collective constant accounting for a number of rate-influencing parameters such as collision frequency, steric factors, molecular orientation, gas concentration, active sites, surface area, etc.

The Arrhenius plots for k_{RPM} versus $1/T$ are shown in Fig. 6. The kinetic parameters, E_a and A_0, were determined from the gradient and y-intercept of the trend lines, respectively. Data from the low temperature measurements up to 900 °C was used to ensure that Regime I kinetics were determined as intended. The transition between Regime I and Regime II kinetic control occurs at the discontinuity in the plots, where a change in gradient is observed.

Some of the parameters encompassed by the pre-exponential factor can be determined and expressed explicitly as additional terms to the Arrhenius equation, allowing their influence on the reactivity to be examined. Analogous experiments were therefore performed at various gas concentrations to determine the reaction order, n, in Eq. (4). The reaction order data are presented graphically in Fig. 7.

$$k = A_0 \exp\left(-\frac{E_a}{RT}\right).[C_g]^n \quad (4)$$

The calculated values for the activation energy, pre-exponential factor and reaction order are presented in Table 6 and discussed in the following.

For char gasification under CO_2 conditions, the calculated activation energy for all samples is comparable, and ranges from 162 to 175 kJ/mol, as shown by the similarity in the slopes of the fitted data. There is a slight but consistent increase for smaller particle sizes, likely due to variation in the distribution of inorganic components over the two particle size ranges, as noted above. The calculated pre-exponential factors vary significantly between coal chars and particle size ranges under CO_2 conditions. In general, A_0 is higher for smaller particles of a given char, indicating that a greater number of successful solid–gas interactions occur during gasification, resulting in a faster gasification rate. Smaller particles were thus determined to be more reactive under these conditions due to their inherently higher surface area.

Within a particular particle size range, the order of increasing char-CO_2 gasification reactivity was Morwell > Yallourn > Loy Yang, which corresponds to the order of increasing pre-exponential factor. The order does not correspond directly to the surface area, porosity, or catalytic inorganic species concentrations of the char samples, indicating that the apparent char reactivity is determined by a combination of these parameters, as they may all influence the magnitude of the pre-exponential factor. This result, in combination with the similarity in the activation energy values, indicates that the dominant influence in the case of CO_2 gasification reactivity of these chars is morphological in nature. The typical, low ash content of the Victorian brown coals also contributes to their similar reactivity under CO_2 conditions, as there is similarly minimal inhibition by extraneous material of the reactive gas's access to remaining active carbon sites at high conversion for all samples.

The order of the reaction with respect to CO_2 concentration was determined for the larger particle size only. The order was similar for all three chars, and ranged from 0.39 to 0.48. A positive value of n shows that increasing the reagent gas concentration will result in an increase in rate, and the variation will be larger for increases at lower concentrations. The higher the reaction order, the less influence a variation in reagent concentration will have on the apparent

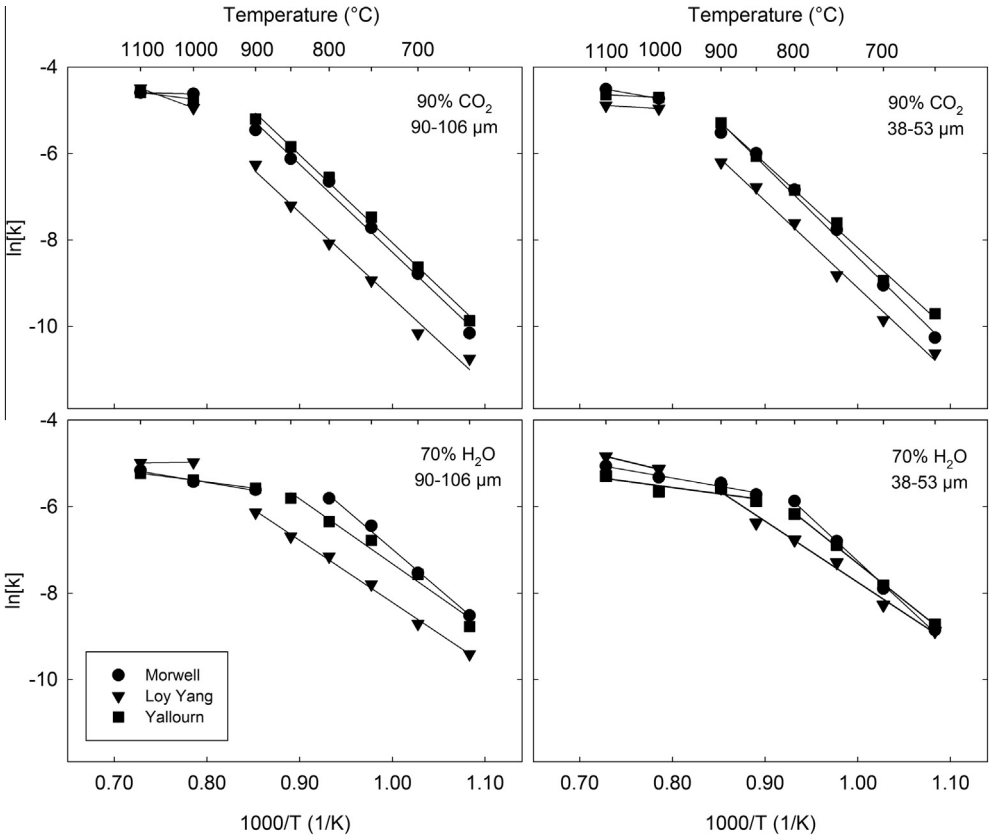

Fig. 6. Arrhenius plots showing the temperature dependence of CO_2 and steam gasification of 38–53 μm and 90–106 μm particle size fractions.

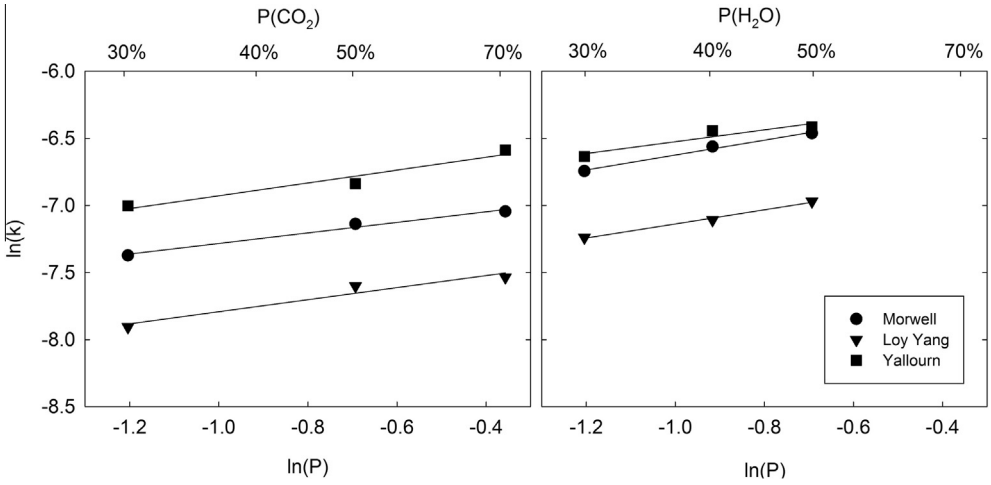

Fig. 7. Dependence of char gasification rate on CO_2 and steam concentration.

gasification rate; therefore a significant influence is indicated by the current results. Previous studies conversely showed an apparent reaction order of 1 for Loy Yang char under CO_2 gasification conditions [32]. It is likely that differing experimental apparatus and sample preparation are responsible for the discrepancy.

Under steam gasification conditions, the char pore structure alters considerably [33], which has a significant effect on char gasification reactivity. Hydrogen radicals produced by the steam gasification mechanism [11] induce condensation reactions, reducing some of the smaller aromatic rings (3–5 carbons) to larger, less reactive structures ($\geqslant$6 carbons), exposing and displacing inorganic species such as Na and Ca, which are known to catalyse the char gasification reactions [34,35]. The effect of inherent catalytic species on steam gasification reactivity involves the interaction between the catalyst, oxygen and carbon via the formation and desorption of the C[O] complex [12]. This may be via direct involvement of the catalyst species in the reaction mechanism, or by indirect enhancement of the affinity of the carbon active site for oxygen. The presence of catalytic inorganic species may therefore increase reactivity by directly reducing the activation energy, by increasing the pre-exponential factor, or both.

For char-steam conditions, the activation energy for all samples is more variable than under CO_2 conditions, and ranges from 119 to 165 kJ/mol. In the case of Morwell char, the similarity in E_a values

Table 6
Kinetic parameters calculated using the random pore model over the range of 10–50% char conversion.

Char sample	Char-CO_2 gasification				Char-steam gasification			
	Activation energy (E_a, kJ/mol)	Pre-exponential (A_0, s^{-1})	Reaction order (n)	Regime I to II transition (°C)	Activation energy (E_a, kJ/mol)	Pre-exponential (A_0, s^{-1})	Reaction order (n)	Regime I to II transition (°C)
Morwell								
90–106 μm	168.96	1.69E+05	0.39	900–1000	152.18	8.25E+04	0.55	750–850
38–53 μm	175.17	3.17E+05	*n.d.*	900–1000	165.33	3.06E+05	*n.d.*	750–850
Yallourn								
90–106 μm	168.82	2.07E+05	0.48	900–1000	134.33	7.14E+03	0.44	800–900
38–53 μm	162.23	8.35E+04	*n.d.*	900–1000	141.98	1.74E+04	*n.d.*	800–900
Loy Yang								
90–106 μm	164.86	3.58E+04	0.44	900–1000	119.24	4.59E+02	0.53	900–1000
38–53 μm	167.29	6.08E+04	*n.d.*	900–1000	117.51	5.94E+02	*n.d.*	900–1000

n.d.: not determined.

under CO_2 and steam conditions indicates that there is little or no difference in catalytic activity under the conditions examined. For both particle sizes of the Loy Yang and Yallourn samples, the activation energy is significantly lower under steam gasification conditions. This difference may be attributed to the known dual catalytic effect of Ca in the presence of Na, which may contribute to differences in both pre-exponential factor and activation energy. CaO is a well-established char gasification catalyst that it is gradually deactivated under steam gasification conditions [36]. However, a synergy exists between Ca and Na in which Na contributes autonomously to the catalysis of the gasification reaction, and also simultaneously enhances the contribution of Ca by inhibiting the agglomeration mechanism [12]. Therefore, the Loy Yang sample exhibits the highest steam gasification reactivity, with the highest combined molar ratio of Na/(Na + Ca) in char, followed by Yallourn. The trend in E_A also closely follows the trend of Na content in the char samples.

There further exists an upper limit to the catalytic effectiveness of increasing amounts of Ca. The relatively low reactivity of Morwell char, similar to that of the CO_2 case, despite the high Ca (+Na) content, is thereby explained by the very low Na content, possibly due to more effective volatilisation in the absence of high Si and Al content.

These results contradict previous studies in which char prepared from Morwell coal showed higher reactivity than that from Loy Yang coal [37]. Disregarding the potential impact of differing experimental methodologies, the sand and clay inclusions in the LY sample used in this study apparently altered the coal composition such that Na and Ca were retained in the char as water soluble silicates, carbonate and sulphates, some of which appear to therefore be available as gasification catalysts under steam conditions. Under pyrolysis conditions at 1000 °C, Na would normally be largely volatilised from this coal [14] and unavailable for catalytic or synergistic activity.

The pre-exponential factors and activation energies for the three char samples under steam gasification conditions follow the opposite trend of increasing reactivity as for CO_2 gasification, Morwell < Yallourn < Loy Yang, indicating that the relative success of collisions between active carbon sites and reagent gas molecules is similar. It is likely that differences in the accessibility of the char structure are therefore responsible for the difference in the pre-exponential factors between samples. The reaction orders for the three chars under steam conditions are also similar to those for CO_2 gasification, although with a slightly wider spread, indicating a similar magnitude of influence of the gas concentration on gasification rate.

Further evidence of the effect of steam gasification on char reactivity is the difference in the Regime I to Regime II transition temperature ranges. Under CO_2 gasification conditions, it appears that the influence of catalytic species was restricted only to the enhancement of active sites in the char matrix as the activation energies and transition temperature ranges were comparable for all samples. In the case of steam gasification, however, there not only appears to be some influence on the reactive sites, but also on the transition temperature ranges for some chars, indicating that mass transfer effects are influential at lower temperatures, potentially due to differences in the reaction mechanism, and hence catalytic reaction pathways, between steam and CO_2.

4. Conclusion

The gasification kinetics of chars prepared from Morwell, Yallourn and Loy Yang Victorian brown coals under rapid pyrolysis conditions were determined by thermogravimetric analysis. The chars were gasified under CO_2 and steam at temperatures between 650 and 1100 °C to determine the temperature dependence of the gasification reactions and the effect of reagent partial pressure. The difference in reaction rate of two particle size ranges was negligible, and the order of increasing char-CO_2 and char-steam gasification reactivity of the three coal chars based on char conversion rate was contradictory. A significant influence of the partial pressure of gasification reagent is indicated by the current results. The dominant influence in the case of CO_2 gasification reactivity of these chars is morphological in nature, while the most significant factor in the case of steam gasification appears to be the concentration of catalytic inorganic species retained during char formation.

Acknowledgements

The authors would like to thank Brown Coal Innovation Australia (BCIA) and the Australian Research Council's Linkage Infrastructure, Equipment and Facilities Scheme (LEIF 120100141) for the funding provided to facilitate this study. Mr. Sean Corcoran and Mr. Vu Dao are also gratefully acknowledged for their assistance in performing TGA experiments and data analysis.

References

[1] U.S. Department of Energy, 2010 Worldwide Gasification Database, (2010).
[2] D.G. Roberts, D.J. Harris, A. Tremel, A.Y. Ilyushechkin, Linking laboratory data with pilot scale entrained flow coal gasification performance. Part 2: pilot scale testing, Fuel Process. Technol. 94 (2012) 26–33.
[3] X. Li, C.-Z. Li, Volatilisation and catalytic effects of alkali and alkaline earth metallic species during the pyrolysis and gasification of Victorian brown coal. Part VIII. Catalysis and changes in char structure during gasification in steam, Fuel 85 (2006) 1518–1525.
[4] A. Molina, F. Mondragón, Reactivity of coal gasification with steam and CO_2, Fuel 77 (1998) 1831–1839.
[5] K. Miura, K. Hashimoto, P.L. Silveston, Factors affecting the reactivity of coal chars during gasification, and indices representing reactivity, Fuel 68 (1989) 1461–1475.

[6] K.H. Van Heek, H.-J. Mühlen, Aspects of coal properties and constitution important for gasification, Fuel 64 (1985) 1405–1414.
[7] N.V. Russell, J.R. Gibbins, J. Williamson, Structural ordering in high temperature coal chars and the effect on reactivity, Fuel 78 (1999) 803–807.
[8] N.M. Laurendeau, Heterogeneous kinetics of coal char gasification and combustion, Prog. Energy Combust. Sci. 4 (1978) 221–270.
[9] O. Senneca, P. Russo, P. Salatino, S. Masi, The relevance of thermal annealing to the evolution of coal char gasification reactivity, Carbon 35 (1997) 141–151.
[10] O. Senneca, P. Salatino, S. Masi, Microstructural changes and loss of gasification reactivity of chars upon heat treatment, Fuel 77 (1998) 1483–1493.
[11] J. Gadsby, C.N. Hinshelwood, K.W. Sykes, The kinetics of the reactions of the steam-carbon system, Proc. R. Soc. London A 187 (1946) 129–151.
[12] Y. Nishiyama, Catalytic gasification of coals — features and possibilities, Fuel Process. Technol. 29 (1991) 31–42.
[13] D.J. Brockway, A.L. Ottrey, R.S. Higgins, Inorganic constituents, in: R.A. Durie (Ed.), The Science of Victorian Brown Coal: Structure, Properties and Consequences for Utilisation, Butterworth Heinemann, 1991, pp. 247–278.
[14] C.Z. Li, C. Sathe, J.R. Kershaw, Y. Pang, Fates and roles of alkali and alkaline earth metals during the pyrolysis of a Victorian brown coal, Fuel 79 (2000) 427–438.
[15] P.L. Walker Jr., F. Rusinko Jr., L.G. Austin, Gas reactions of carbon, in: D.D. Eley, P.W. Selwood, P.B. Weisz (Eds.), Advances in Catalysts, vol. XI, Academic Press, New York, 1959, pp. 133–221.
[16] A. Tremel, T. Haselsteiner, C. Kunze, H. Spliethoff, Experimental investigation of high temperature and high pressure coal gasification, Appl. Energy 92 (2012) 279–285.
[17] A. Cuadrat, A. Abad, F. García-Labiano, P. Gayán, L.F. de Diego, J. Adánez, Relevance of the coal rank on the performance of the in situ gasification chemical-looping combustion, Chem. Eng. J. 195–196 (2012) 91–102.
[18] W. Huo, Z. Zhou, F. Wang, G. Yu, Mechanism analysis and experimental verification of pore diffusion on coke and coal char gasification with CO_2, Chem. Eng. J. 244 (2014) 227–233.
[19] J. Tanner, K.B. Kabir, M. Müller, S. Bhattacharya, Low temperature entrained flow pyrolysis and gasification of a Victorian brown coal, Fuel 154 (2015) 107–113.
[20] D.G. Roberts, D.J. Harris, Char gasification in mixtures of CO_2 and H_2O: competition and inhibition, Fuel 86 (2007) 2672–2678.
[21] P. Ollero, A. Serrera, R. Arjona, S. Alcantarilla, Diffusional effects in TGA gasification experiments for kinetic determination, Fuel 81 (2002) 1989–2000.
[22] G.Q. Lu, D.D. Do, Comparison of structural models for high-ash char gasification, Carbon 32 (1994) 247–263.
[23] J. Gadsby, F.J. Long, P. Sleightholm, K.W. Sykes, The mechanism of the carbon dioxide-carbon reaction, Proc. R. Soc. London A 193 (1948) 357–376.
[24] T. Adschiri, T. Shiraha, T. Kojima, T. Furusawa, Prediction of CO_2 gasification rate of char in fluidized bed gasifier, Fuel 65 (1986) 1688–1693.
[25] J.L. Johnson, Kinetics of bituminous coal char gasification with gases containing steam and hydrogen, in: L.G. Massey (Ed.), Coal Gasification, American Chemical Society, 1974, pp. 145–178.
[26] S. Dutta, C.Y. Wen, R.J. Belt, Reactivity of coal and char. 1. In carbon dioxide atmosphere, Ind. Eng. Chem. Process Des. Dev. 16 (1977) 20–30.
[27] M. Tomaszewicz, G. Łabojko, G. Tomaszewicz, M. Kotyczka-Morańska, The kinetics of CO_2 gasification of coal chars, J. Therm. Anal. Calorim. 113 (2013) 1327–1335.
[28] A. Gomez, R. Silbermann, N. Mahinpey, A comprehensive experimental procedure for CO_2 coal gasification: Is there really a maximum reaction rate?, Appl Energy 124 (2014) 73–81.
[29] S.K. Bhatia, D.D. Perlmutter, A random pore model for fluid-solid reactions: I. Isothermal, kinetic control, AIChE J. 26 (1980) 379–386.
[30] D.J. Harris, I.W. Smith, Intrinsic reactivity of petroleum coke and brown coal char to carbon dioxide, steam and oxygen, Symp. (Int.) Combust. 23 (1991) 1185–1190.
[31] T.F. Wall, G.-S. Liu, H.-W. Wu, D.G. Roberts, K.E. Benfell, S. Gupta, J.A. Lucas, D.J. Harris, The effects of pressure on coal reactions during pulverised coal combustion and gasification, Prog. Energy Combust. Sci. 28 (2002) 405–433.
[32] T.-W. Kwon, S.D. Kim, D.P.C. Fung, Reaction kinetics of char—CO_2 gasification, Fuel 67 (1988) 530–535.
[33] H.-L. Tay, S. Kajitani, S. Zhang, C.-Z. Li, Effects of gasifying agent on the evolution of char structure during the gasification of Victorian brown coal, Fuel 103 (2013) 22–28.
[34] P. Nanou, H.E. Gutiérrez Murillo, W.P.M. van Swaaij, G. van Rossum, S.R.A. Kersten, Intrinsic reactivity of biomass-derived char under steam gasification conditions-potential of wood ash as catalyst, Chem. Eng. J. 217 (2013) 289–299.
[35] N. Ellis, M.S. Masnadi, D.G. Roberts, M.A. Kochanek, A.Y. Ilyushechkin, Mineral matter interactions during co-pyrolysis of coal and biomass and their impact on intrinsic char co-gasification reactivity, Chem. Eng. J. 279 (2015) 402–408.
[36] L.R. Radović, P.L. Walker Jr, R.G. Jenkins, Effect of lignite pyrolysis conditions on calcium oxide dispersion and subsequent char reactivity, Fuel 62 (1983) 209–212.
[37] T. Takarada, Y. Tamai, A. Tomita, Reactivities of 34 coals under steam gasification, Fuel 64 (1985) 1438–1442.